Atmospheric Environment 298 (2023) 119613

Contents lists available at ScienceDirect

Atmospheric Environment

journal homepage: www.elsevier.com/locate/atmosenv

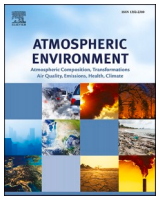

Deriving composition-dependent aerosol absorption, scattering and extinction mass efficiencies from multi-annual high time resolution observations in Northern France

A. Velazquez-Garcia [a,b,**], S. Crumeyrolle [b,*], J.F. de Brito [a], E. Tison [a], E. Bourrianne [b], I. Chiapello [b], V. Riffault [a]

[a] IMT Nord Europe, Institut Mines-Télécom, Université de Lille, Centre for Energy and Environment, 59000, Lille, France
[b] LOA-Laboratoire d'Optique Atmosphérique, CNRS, UMR 8518, Univ. Lille, 59000, Lille, France

HIGHLIGHTS

- High time resolution in situ measurements from a French suburban ACTRIS site.
- Ammonium nitrate dominates the PM_1 fraction during spring.
- Low average value of the Single Scattering Albedo in PM_1 at 0.77
- Carbonaceous aerosols dominate (50%) the extinction in the visible range.
- Organics contribute 22% to absorption in the near UV-range.

ARTICLE INFO

Keywords:
PM_1
Urban sites
Optical properties
Chemical properties
Aerosol mass efficiencies
Brown carbon

ABSTRACT

The wide range of sources and complex (trans)formation processes of aerosol particles lead to strong spatial and temporal variability in their physical, chemical and optical properties. Their accurate representation is essential to assess their impacts, notably on climate. Here, we investigate for the first time the aerosol optical properties and their relation to fine particle chemical composition in Northern France, based on a multi-annual in situ dataset. Real-time submicron aerosol measurements at the ATOLL (ATmospheric Observations in liLLe) site have shown that ammonium nitrate contributes about 36% of the total mass, being the predominant species regarding the extinction at 525 nm (35%). Yet, organics are responsible for 22% of the absorption in the UV range (370 nm), pointing at a significant contribution of Brown Carbon. Furthermore, our study highlights the need for site-specific values to correctly assess the impact of different aerosol species on extinction. It also sheds a light on the relevancy of widespread combined aerosol chemical and physical observations to better estimate their role on climate, particularly reducing uncertainties on future scenarios based on mitigation strategies.

1. Introduction

Aerosol particles can influence the Earth's climate through scattering and absorption of solar radiation (Aerosol-Radiation Interactions, ari), as well as affecting cloud formation and lifetime (Aerosol-Cloud Interactions, aci) (Forster et al., 2021; Myhre et al., 2013; Wilcox, 2012). Both the magnitude and sign of these impacts depend mainly on their optical, chemical and microphysical properties (Seinfeld and Pandis, 2012). Light-absorbing carbon and some minerals are the most common particle components that absorb light while all particles scatter light, which contributes the most to extinction. According to estimations of radiative forcing due to ari (RFari) from AeroCom Phase II (Myhre et al., 2013), there is a higher uncertainty on the RFari species breakdown than considering total RFari, e.g. calculations probably underestimate the positive RFari from Black Carbon (BC) and the negative forcing from organic aerosols (OA), and currently there is no evidence that one of these opposing biases dominates over the other.

Total aerosol light extinction, and the contribution for each species

* Corresponding author.
** Corresponding author. IMT Nord Europe, Institut Mines-Télécom, Université de Lille, Centre for Energy and Environment, 59000, Lille, France.
E-mail addresses: ale-vg13@hotmail.com (A. Velazquez-Garcia), suzanne.crumeyrolle@univ-lille.fr (S. Crumeyrolle).

https://doi.org/10.1016/j.atmosenv.2023.119613
Received 29 April 2022; Received in revised form 21 December 2022; Accepted 23 January 2023
Available online 26 January 2023

can be assessed using the volume average mixing (VAM) model and a priori Mass Extinction Efficiency (MEE) values for different species (Hand and Malm, 2007). MEE can be derived whether theoretically (calculations using refractive index from literature and measured size distribution) (Cheng et al., 2008) or experimentally (Wang, 2015a) for each chemical compound. Such methods have originally been proposed within the Interagency Monitoring of Protected Visual Environments (IMPROVE) program, applied for long-term measurements and at first on measurements performed over the USA national parks (Malm et al., 1994; Pitchford et al., 2007). Subsequently, the method has been applied in other parts of the world, including China (Chen et al., 2016; Cheng et al., 2008; Z. Cheng et al., 2015; Qu et al., 2015; Tao et al., 2020; Wang et al., 2015a,b; Wang et al., 2015a,b; Xia et al., 2017; Yao et al., 2010; Zhou et al., 2019) and, to a lesser extent, some south European sites mainly in Italy, Spain, and Greece (Sciare et al., 2005; Titos et al., 2012; Valentini et al., 2018; Vecchi et al., 2018). However, to the best of our best knowledge, the IMPROVE approach, although most useful to reduce uncertainties associated to the relation between aerosol chemical composition and their optical properties, has not been investigated in the polluted urban background environments of northwestern European countries. Besides, instrumentation capable of measuring aerosol chemical composition with high time resolution allows nowadays for a detailed view of the variability of physical and chemical coupling over a time scale of minutes, while still providing multi-annual observations. Precise estimates of composition-dependent MEEs would therefore significantly improve estimates of the role of different aerosol compounds on visibility, which is particularly relevant for places identified as pollution hotspots.

The north of France suffers from significant particulate pollution events, arising from a combination of heavily populated urban areas, industrial/agricultural/shipping emissions and transport of polluted atmospheric plumes from the UK, Belgium, Germany and Eastern Europe (Crumeyrolle et al., 2021; Rodelas et al., 2019; Waked et al., 2018). Here, we use three years of online submicron aerosol (PM_1) surface measurements at a suburban site in Lille to derive composition-dependent Mass Scattering Efficiencies (MSE), Mass Absorption Efficiency (MAE), and Mass Extinction Efficiency (MEE) at different wavelengths, and thus assess the contribution of each of the main species on optical properties in the region. The proposed analysis presents several advantages, including a highly time-resolved chemical information capturing fast processes of aerosol dynamics. However, it is important to note that aerosol species such as dust or sea salt are not considered here. This is partly overcome by focusing on PM_1 fraction, and by removing periods of identified influence of those species, nonetheless limitations remain. More fundamentally, an assumption inherent to VAM is that aerosol population is externally mixed (independent contribution to extinction), and its MEE is constant despite changes on aerosol size distribution. Despite those assumptions, VAM has successfully provided similar and more stable results than complex mixing rules (e.g. Maxwell Garnett, Bruggeman theory, core-shell model) for retrieving aerosol components (Li et al., 2019; Wang et al., 2021).

2. Material and methods

Sampling site. Since October 2014 near real-time in situ measurements are performed routinely on the ATOLL (ATmospheric Observations in liLLe) platform located on the rooftop of a University of Lille building (50.6111 °N, 3.1404 °E, 70 m a.s.l.), 6 km south east of Lille downtown area, without significant local aerosol sources (Riffault et al. *in preparation*). With more than 1.1 million inhabitants, the metropolitan area of Lille is characterized by a high population density (1765 inhabitants km^{-2}). As part of North of France, bounded on the north by the Benelux countries, the sampling site is under the influence of various anthropogenic regional and trans-boundary emission sources that cause relatively frequent particulate pollution episodes exceeding the WHO threshold values (Waked et al., 2018). The ATOLL site is part of the CARA program (Favez et al., 2021) and a French National Facility of the European 'Aerosols, Clouds, and Trace gases Research Infrastructure' (ACTRIS) network focusing on high-quality long-term atmospheric data.

The chemical composition of non-refractory submicron particles ($NR\text{-}PM_1$) has been continuously monitored using an Aerosol Chemical Speciation Monitor (ACSM, Aerodyne Research Inc.) providing mass concentrations of particulate organics (Org), nitrate (NO_3^-), sulfate (SO_4^{2-}), ammonium (NH_4^+) and chloride (Cl^-) (Ng et al., 2011). Equivalent Black carbon (eBC) concentrations and the absorption coefficients (σ_{abs}) are continuously measured with a seven-wavelength aethalometer (AE33, Magee Scientific Inc.) (Cuesta-Mosquera et al., 2021; Drinovec et al., 2015). According to ACTRIS current guidelines (https://actris-ecac.eu/particle-light-absorption.html), σ_{abs} coefficients at each wavelength have been recalculated by multiplying eBC by the mass-specific absorption coefficient (MAC) then dividing by the suitable harmonization factor to account for the filter multiple scattering effect, 2.21 (M8020 filter tape) in 2017 and 1.76 (M8060 filter tape) for 2018 and 2019. These two instruments have independent sampling lines. The ACSM is downstream a $PM_{2.5}$ cyclone (URG-2000-30ED, URG Corp.) at 3 L min^{-1} and a Nafion dryer with stainless steel tubing (2.3 m) all along. The Aethalometer is working at 5 L min^{-1} downstream a PM_1 cyclone (BGI SCC1.197, Mesa Labs) with a stainless-steel line (2.6 m) and flexible tubing (1.85 m) designed to limit the aerosol electrostatic losses.

Dry scattering coefficient (σ_{scat}) measurements are performed using two Aurora (ECOTECH) nephelometers (4000 and 3000) operating at 450, 525, and 635 nm. Both nephelometers are running in series, with a Nafion dryer upstream of both instruments (<40% RH), and a PM_1 cyclone prior the Aurora 3000. Therefore, dry scattering coefficients are measured first within the total suspended particle (A-4000) then within the PM_1 (A-3000) fractions. Both nephelometers are calibrated daily using filtered air and weekly using CO_2. Both scattering coefficients have been corrected from angular truncation errors and illumination intensity non-idealities based on Müller et al. (2011).

All the data have been averaged to the ACSM time stamp (i.e. about 30 min), and cover the period from July 2017 to December 2019. The optical properties, that is to say the extinction coefficient (σ_{ext}) – explained later on in this section – and the Single Scattering Albedo (SSA_{PM1}) defined in eq. (1) below, were estimated at the three nephelometer wavelengths. Therefore, the absorption coefficient at wavelength λ ($\sigma_{abs,\lambda}$) was interpolated using the Ångström Absorption Exponents (AAE) calculated every 30 min (for each data point) using the nearest wavelengths ($AAE_{370\text{-}470}$ for $\sigma_{abs,450}$ calculations; $AAE_{520\text{-}590}$ for $\sigma_{abs,525}$ calculations; $AAE_{590\text{-}660}$ for $\sigma_{abs,635}$ calculations).

$$SSA_\lambda = \frac{\sigma_{scat,\lambda}}{\sigma_{abs,\lambda} + \sigma_{scat,\lambda}} \quad \text{eq. 1}$$

Further technical details of the sampling are given in Table S1, and data coverage on Fig. S1.

Light extinction retrieval. The extinction coefficient at a given wavelength λ can be expressed as the sum of scattering and absorption coefficients of particles and gases in the atmosphere:

$$\sigma_{ext,\lambda} = \sigma_{ap,\lambda} + \sigma_{sp,\lambda} + \sigma_{ag,\lambda} + \sigma_{sg,\lambda} \quad \text{eq. 2}$$

where subscripts "s" and "a" indicate scattering and absorption, and "p" and "g" denote particles and gases, respectively. NO_2 is the main absorbing gas within the visible range and its absorption can be directly estimated by multiplying its concentration by its absorption efficiency (0.33) (Pitchford et al., 2007). Scattering by gases is described by the Rayleigh scattering (RS) theory, which can be estimated using local meteorological conditions (T and RH) (Bodhaine et al., 1999).

Regarding particles, the U.S. IMPROVE program proposed a mathematical expression which allows the individual particle component contributions to the extinction coefficient to be separately estimated by multiplying the concentrations (C) of six major components (j) with

typical component- and site-specific mass extinction efficiencies (MEE). The formula also includes a water growth factor as a function of relative humidity (f(RH)) for hygroscopic species. Thus, the extinction coefficient can be calculated by:

$$\sigma_{ext,\lambda} = \sum_j MEE_{j,\lambda} \times f(RH)_j \times C_j + RS_\lambda + \sigma_{NO_2,\lambda} \quad \text{eq. 3}$$

IMPROVE, based on filter analysis, suggested fixed MEE values for six major chemical species of $PM_{2.5}$ including ammonium sulfate (AS), ammonium nitrate (AN), organics (Org), black carbon (BC), fine soil (FS) and sea salt (SS). Yet, MEE values vary depending on site (Hand and Malm, 2007), season (Tao et al., 2014) and particle morphology (Cheng et al., 2008). Therefore, the application of such coefficients at different sites with no local tailoring can lead to significant uncertainties (Valentini et al., 2018). Contrasting IMPROVE, in this analysis we employed online measurements performed under dry conditions, thus the water growth factor is set to be equal to 1. Besides, this work does not consider the contribution of gases to optical properties, only for aerosol particles. Indeed, the nephelometer is calibrated daily for a zero adjustment. This calibration is performed by sampling particle free air (filtered using HEPA filter) so that only gases can enter the instrument. The remaining signal is then corresponding to the Rayleigh scattering and is set to zero automatically. Assuming that the Rayleigh signal remains constant for the whole day, the signal acquired by the nephelometer is thus only corresponding to the particle scattering. On the other hand, the attenuation measured over time by the aethalometer can be only influenced by particles. This attenuation in time is then converted by a corresponding light-absorbing aerosol concentration in the atmosphere Thus, the equation employed here is expressed as:

$$\sigma_{ext,\lambda} = \sum_j MEE_{j,\lambda} \times C_j \quad \text{eq. 4}$$

In this work, we retrieved local composition-dependent MSE, MAE, and MEE values through Multiple Linear Regression (MLR) taking the optical properties measured (σ_{scat}, σ_{abs}) as independent variables and, the species mass concentrations (C_j) as dependent variables. Calculations were performed using the least square method, coefficients were constrained to be positive to retain their physical meaning, and the linear intercept was fixed to zero to force PM_1 species to explain all PM_1 scattering and absorption coefficients. With this method, MEEs have been estimated for each species over the whole period of three years, encompassing clean and polluted conditions. The equation of MLR employed in this work is written in eq. (5):

$$y = \sum_i b_i x_i + \varepsilon \quad \text{eq. 5}$$

where y is the output data to be predicted by the model (here extinction, absorption or scattering coefficients), x_i are independent input variables (here the mass concentration of particulate chemical species), b_i, the linear regression constants (here MEE, MAE and MSE), and ε the residuals.

The MLR analysis (RMSE:15.2; bias: 1.5) was performed in MATLAB 2020a on almost 18,000 points of ~30-min averaged PM_1 chemical composition (NR-PM_1 and eBC) and optical coefficients (σ_{scat}, σ_{abs}) during the whole period of interest. Days flagged as impacted by desert dust events at the ATOLL platform were removed from the dataset to avoid possible errors, leading to the exclusion of 3% of data, mostly around March 2019. To evaluate the robustness of the MLR method used in this study, the residuals as well as the fractional bias were introduced (see Supplementary material). During 3 full years of measurements corresponding to more than 18,000 data points, 94% of the standardized residuals are obtained within an interval of 2σ around zero while only 6% are highlighted as outliers. Therefore, the MLR analysis developed here is robust and the results will be interpreted in the next section.

3. Results & discussion

Aerosol properties. At the ATOLL site, the 3-year averaged PM_1 concentration (calculated as the sum of ACSM species and BC concentrations) and its standard deviation is 14.2 ± 9.7 μg m^{-3}, with seasonal averages of 16.4 ± 9.5, 15.5 ± 10.6, 14.0 ± 9.3 and 11.3 ± 8.8 μg m^{-3} for winter, spring, fall and summer, respectively. Fig. 1 shows the monthly averages of the PM_1 species concentrations. Although PM_1 changes significantly throughout the year, individual species exhibit varied behaviors. Sulfate evolution did not show a marked seasonality, with averaged monthly values varying between 0.7 ± 0.7 μg m^{-3} (winter - DJF) and 0.9 ± 0.6 μg m^{-3} (summer - JJA). Concentrations of particulate sulfate could be directly emitted via some natural (volcanoes, oceanic phytoplankton) and anthropogenic (coal and oil combustion) sources or secondarily formed through the oxidation of its gaseous precursor sulfur dioxide (SO_2). In France emissions of SO_2 are mainly attributed to energy transformation, manufacturing, industry and residential or tertiary emissions, therefore concentrations can be highly variable at a given site, depending on the presence of local emitters and air mass origins (Rodelas et al., 2019). Moreover, non-refractory Cl^- is found typically below the detection limit, representing a minor fraction of PM_1 (<1%), with concentrations close to zero over the entire observation period.

Ammonium (NH_4^+), nitrate (NO_3^-) and carbonaceous aerosols (Org, BC) variations are more season-dependent (Fig. 1). Carbonaceous aerosols showed a higher concentration in winter (5.3 ± 4.9 and 1.2 ± 1.2 μg m^{-3} for Org and BC, respectively) compared to summer (3.7 ± 3.4 to and 0.7 ± 0.5 μg m^{-3}). The increase in carbonaceous aerosols during winter could be explained by residential heating emissions combined with stagnant conditions, also favorable for semi-Volatile Organic Compounds (VOCs) species to be in particle-phase. On the other hand, during summer, Org concentrations are significantly impacted by secondary formation (SOA) (Laskin et al., 2015; Zhang et al., 2020). The concentrations of NH_4^+ and NO_3^- exhibit a marked seasonal variation showing maximum during spring with average peaks around 2.2 ± 1.8 μg m^{-3} and 4.5 ± 4.8 μg m^{-3}. The seasonality of those species arises from the widespread use of fertilizers (rich in ammonia) in the agricultural sector in spring, associated with combustion processes from traffic or industry (main source of NOx at urban sites) (Rodelas et al., 2019), compounded with favorable meteorological conditions. The

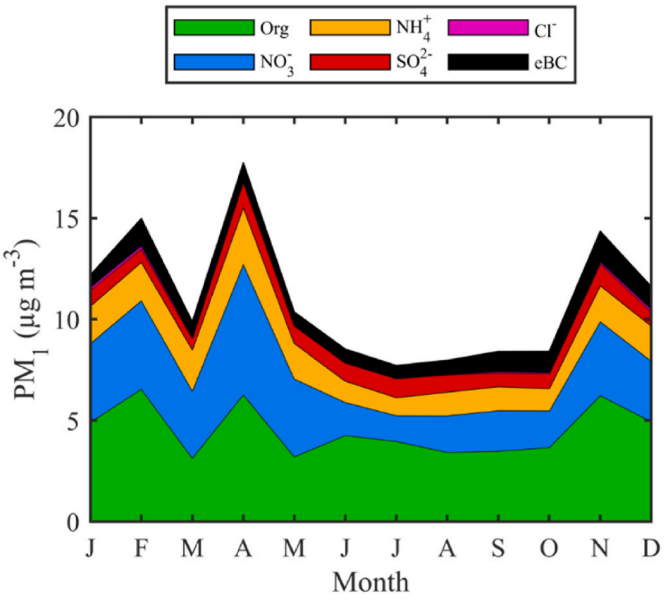

Fig. 1. Monthly averages of PM_1 species measured at ATOLL from July 2017 to December 2019.

levels of AN in the HdF region are related to both local and regional origins. Previous studies (Rodelas et al., 2019; Rodelas et al., 2019; Zhang et al., 2021) identified significant contributions of AN and organic aerosols from air masses that passed over Belgium, the Netherlands and Germany (North to North-East sectors) associated to high wind speeds and increased farming activities in those areas, suggesting the transport of neutralized and aged aerosols.

Regarding optical properties in ATOLL, the average light extinction of PM_1 at 525 nm ($\sigma_{ext,525nm}$) is 38.0 ± 34.9 Mm^{-1} consistent with the recent analysis (Laj et al., 2020) performed within the Global Atmosphere Watch (GAW) aerosol network for urban and suburban sites in Europe. For instance, in the urban Ispra, Italy (IPR), the total extinction value of the $PM_{2.5}$ fraction (44.8 Mm^{-1}) is comparable to the extinction observed here, although it is important to note differences in cut-off sizes (1 μm vs 2.5 μm). Seasonal variations of extinction coefficient show a marked increase during winter (55.5 ± 39.9 Mm^{-1}) compared to summer (28.2 ± 27.0 Mm^{-1}), a trend that was also seen in Italy.

Fig. 2 depicts the PM_1 chemical composition as a function of SSA_{PM1}, i.e., the ratio of scattering to extinction coefficients, at 525 nm. In general, periods dominated by highly absorbing aerosols, corresponding to low SSA_{PM1} values (<0.60) where carbonaceous aerosols dominate the chemical composition with over 75% of the mass concentration. Conversely, SSA_{PM1} increases correspond to significant increases of the relative contribution of Secondary Inorganic Aerosols (AS and AN, particularly the latter). The mean SSA_{PM1} observed at ATOLL is 0.77 ± 0.11, exhibiting values comparable to most urban sites in Europe including Ispra, and lower than most remote sites (Laj et al., 2020).

Composition-dependent optical properties. The composition- and wavelength-dependent MSE, MAE and MEE parameters retrieved through the MLR approach applied to PM_1 measurements at the ATOLL site are summarized in Table 1. For all components, the UV and blue ranges are characterized by the largest mass extinction, scattering and absorption efficiencies, which decrease at higher wavelengths. MEE values retrieved in northern France are compared to a comprehensive list of composition-dependent MEEs found in the literature (Table S2). Focusing on results from comparable approaches (MLR for species in PM_1), in Shenzhen, China (Yao et al., 2010) the MEE value of AS at 550 nm retrieved is 2.3 $m^2\ g^{-1}$, whereas we obtained 5.0 $m^2\ g^{-1}$ at 525 nm. Conversely, their MEE for Organics was 4.5 $m^2\ g^{-1}$, while we obtained 1.8 $m^2\ g^{-1}$ at ATOLL. Another study (Wang et al., 2015a,b) also applied MLR to PM_1 measurements performed in Beijing (China), and obtained

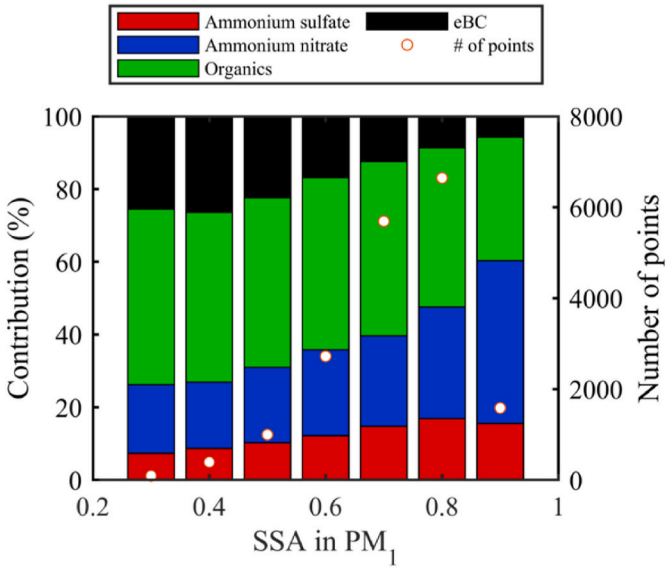

Fig. 2. PM_1 fractional composition (left axis) and number of observations (dots, right axis) according to SSA_{PM1} bins at 525 nm at ATOLL.

values of MEE at 630 nm for AS slightly higher (5–2.7 $m^2\ g^{-1}$) than the value of 4.5 $m^2\ g^{-1}$ at ATOLL (Table 1). Considering the results above were obtained focusing on the same aerosol size fraction, and through similar methodology, those variations can be attributed to difference in aerosol populations, notably their mixing state and species size distributions, ultimately influencing their optical properties (Cheng et al., 2008; Hand and Malm, 2007; Pitchford et al., 2007; Valentini et al., 2018).

Based on $PM_{2.5}$ filter analysis during wintertime in the Po valley, Italy (Valentini et al., 2018), obtained an MEE at 550 nm for AS comparable to ours (4.4 $m^2\ g^{-1}$), but a value almost 3-fold higher for Organics (6.1 $m^2\ g^{-1}$). It is important to mention that organics are characterized by complex chemical composition and optical properties, determined by their origins (anthropogenic or biogenic, primary emitted or secondary produced) (Laskin et al., 2015). The study in Italy (Valentini et al., 2018) focused on a bigger size fraction (1 μm vs 2.5 μm) during a single season (winter), whereas our study targets the PM_1 fraction on a multi-annual basis. Thus, different MEE for organics could be explained by diverse aerosol origins during the studied period (multi-seasonal vs wintertime) with different mixing states and size ranges (Hand and Malm, 2007), although the roles of possible measurement artifacts (ACSM vs Thermal Optical Transmittance analysis) and of the method employed to retrieve aerosol mass efficiency (experimental vs theoretical) cannot be excluded. Indeed, site-specific dry mass extinction efficiencies in the Po valley (Valentini et al., 2018) were retrieved considering additional physical properties (e.g. density, geometric mean radii and the mass fractions of four modes). For organics, the average ambient dry mass size distribution used (Bernardoni et al., 2017) also contemplates hygroscopicity for water-soluble organics, which represents 25% of fine organic carbon concentration. Hence, the discrepancy in MEE calculated for Org is also likely to be ascribed to differences in mass relative contribution and in geometric standard deviations of the modes, as well as the water growth factors detected at the Po Valley compared to ATOLL site.

Fig. 3 displays the impact of using literature values for MEEs with ATOLL mass concentration observations for each species to retrieve the extinction coefficients (eq. (4)). For comparison, we selected six studies focusing on fine aerosol fractions (either 1 or 2.5 μm) and on the same species as in our work (AN, AS, Org, eBC). Using literature values instead of site-specific MEE leads to a large range of reconstructed extinction coefficients at 525 nm. For example, using MEE values based on theoretical calculations (Cheng et al., 2008; Pitchford et al., 2007), could result in a 30% underestimation and 74% overestimation of the total extinction, respectively. Conversely, experimentally-derived MEEs from field observations (Wang et al., 2015a,b; Yao et al., 2010) were within 18% of the total extinction observed here. Nevertheless, even a good agreement for total extinction coefficient does not automatically imply a similar agreement for individual species, as discussed in the next section.

Chemical contribution to the Aerosol Optical Properties (AOPs). By considering the obtained MEEs and average mass concentration of each species, we could calculate their relative contribution to optical properties. Secondary Inorganic Aerosols (SIA), i.e. AN and AS, were the main contributors (67%) to the light scattering for all three wavelengths: 450, 525 and 635 nm (Fig. 4a). Conversely, light absorption is entirely apportioned to carbonaceous aerosols, with Organics being optically active at the near-ultraviolet and blue wavelengths (370–590 nm) accounting up to 22% of the total absorption, the rest being apportioned to eBC (Fig. 4b). This is comparable with what is reported for Zurich in Switzerland (Moschos et al., 2020), for which an Organics contribution to the total measured absorption of 30 ± 14% was assessed at 370 nm, decreasing down to 4 ± 2% at 590 nm, while BC contribution was estimated two-thirds of the particle absorption in the near-UV to infrared wavelength range. Considering aerosol light extinction at 525 nm (Fig. 4c), AN is the dominant species (35%), followed by eBC (29%) and Organics (21%), and finally AS (15%). For other wavelengths, Organics and eBC exhibit a slightly higher contribution at 450 and 635 nm,

Table 1
Retrieved values of Mass Scattering, Absorption and Extinction Efficiencies (MSE, MAE, MEE, respectively) from 370 to 930 nm based on MLR analysis at ATOLL.

	Wavelength (nm)	Ammonium Sulfate	Ammonium Nitrate	Organics	eBC
Mass Scattering Efficiency, MSE ($m^2\ g^{-1}$)	450	7.1	4.6	3.1	–
	525	5.7	3.6	2.2	–
	635	4.8	2.7	1.5	–
Mass Absorption Efficiency, MAE ($m^2\ g^{-1}$)	370	–	–	0.7	11.6
	470	–	–	0.3	8.9
	520	–	–	0.2	7.5
	590	–	–	0.2	6.5
	660	–	–	0.1	5.5
	880	–	–	0.0	3.9
	950	–	–	0.0	3.7
Mass Extinction Efficiency, MEE ($m^2\ g^{-1}$)	450	5.8	4.6	2.9	13.5
	525	5.0	3.7	1.8	11.2
	635	4.5	2.7	1.0	10.3

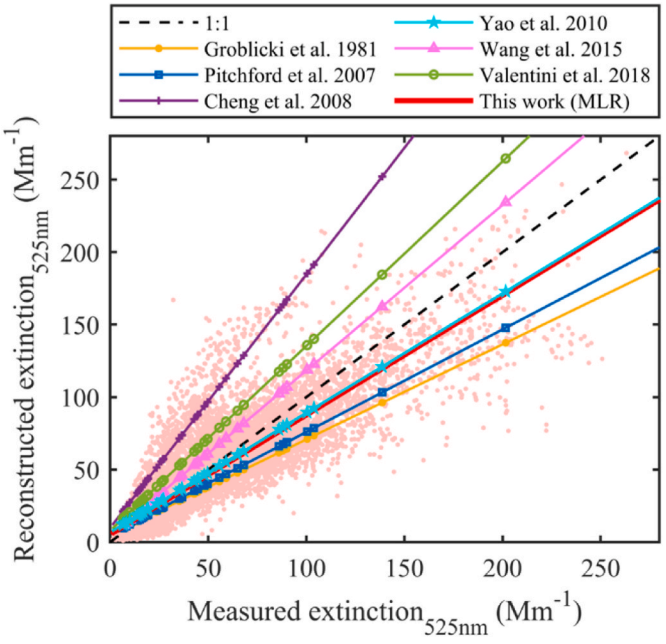

Fig. 3. Scatter plot of reconstructed versus measured aerosol extinction coefficient at 525 nm for ~ 3-year measurements at the ATOLL platform. Solid lines represent the linear least-square fit through the data where y-values have been calculated using fixed MEE taken from the literature (Cheng et al., 2008; Groblicki et al., 1981; Pitchford et al., 2007; Valentini et al., 2018; Wang et al., 2015a,b; Yao et al., 2010) combined with ATOLL PM_1 species mass concentrations. Results of the Multiple Linear Regression with ATOLL MEE values are represented by the pink dots and the solid line in red (# of points: 18,065; R^2: 0.80; slope: 0.82)(For interpretation of the references to colour in this figure legend, the reader is referred to the web version of this article).

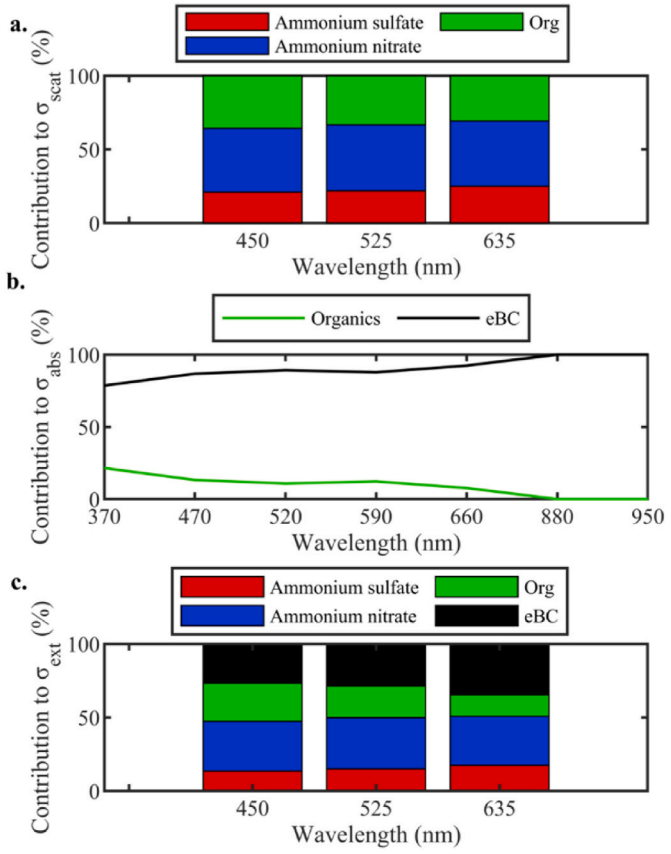

Fig. 4. Averaged relative contributions of PM_1 chemical species to the Aerosol Optical Properties at ATOLL over the period July/2017–December/2019: a) Secondary Inorganic Aerosols and Organics to light scattering at 450, 525 and 635 nm; b) carbonaceous aerosols to light absorption from 370 to 940 nm; c) PM_1 species to light extinction at 450, 525 and 635 nm.

respectively (Fig. 4c). While (Valentini et al., 2018) have also identified AN as the main contributor to extinction at 550 nm in the Po valley (Yu et al., 2010), identified BC (76%) as the dominant species in urban areas in the Pearl River region (China). This highlights the complex and probably mixed influence of source intensities, topography and meteorological conditions that drive light extinction at a given site, and more generally reflects the spatial and temporal variability of fine particles in the atmosphere.

Fig. 5a represents the monthly light extinction broken down according to species contribution, a product of mass efficiency and changes in the mass concentrations. As expected, light extinction is generally higher during the cold months, with three maxima in November, February and April. These months are strongly impacted by aerosol emissions related to solid fuel combustion from residential heating (carbonaceous aerosols), and agricultural activities leading to strong AN ($5.8 \pm 6.2\ \mu g/m^{-3}$) formation (Crenn et al., 2017; Rodelas et al., 2019; Rodelas et al. 2019) during spring. Fig. 5b shows the monthly evolution of the normalized extinction, highlighting the highest contribution of eBC and AN in October and April respectively. AS ($1.2 \pm 1.2\ \mu g/m^{-3}$) has a fairly constant absolute contribution throughout the year peaking at about 25% of extinction during the summer. It is interesting to notice the increase in Organics relative contribution during summertime, likely associated with biogenic particulate secondary formation (Gómez-González et al., 2012) favored at higher temperatures.

As previously discussed, literature-based MEEs yield to strong variability in the reconstructed extinction coefficient. In recent years, MEE

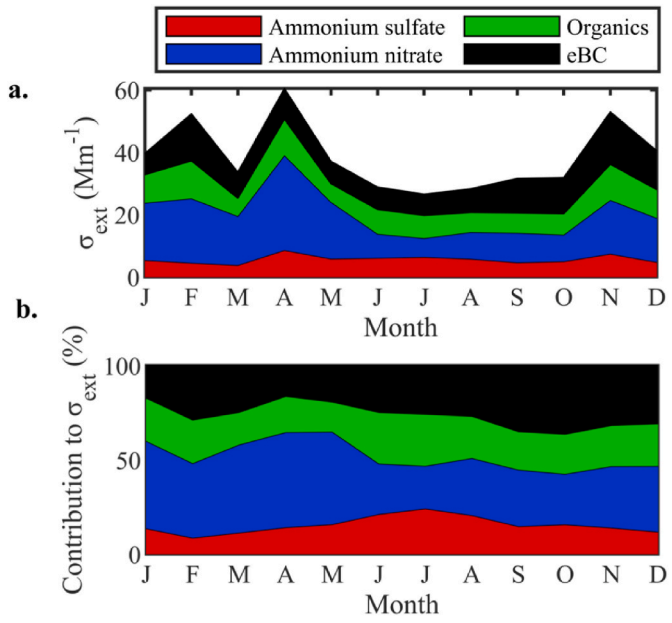

Fig. 5. Contribution of the main aerosol species to the extinction coefficient at ATOLL over the period July 2017–December 2019. a) Monthly-averaged variation of the light extinction coefficient at 525 nm (in Mm^{-1}) for each considered species. b) Monthly-averaged relative contributions of each particulate component to the light extinction coefficient at 525 nm.

estimation via the IMPROVE approach has been applied in numerous studies, mainly carried out at heavily polluted urban areas in China, or over US national parks where uniform haze occurred often. Over Europe, the IMPROVE approach has only been used over south Europe (Sciare et al., 2005; Titos et al., 2012; Valentini et al., 2018; Vecchi et al., 2018). Although the cut-off sizes (1 vs 2.5 μm) and method to derive site-specific MEE are slightly different from this work, we used the only available study for a hotspot of pollution at a European urban site in the Po Valley, Italy (Valentini et al., 2018).

It is important to consider that even for cases when the total extinction is comparable, large discrepancies can remain on composition-based apportionment. For example, applying the MEEs derived from the study of experimental method in Shenzhen for the PM_1 fraction (Yao et al., 2010) to ATOLL mass concentrations reconstructs the total extinction within 18% of the observed values, however it overestimates the role of Organics by 50% compared to similar calculations using ATOLL site-specific MEE (Fig. S2). Conversely, using MEEs, based on theoretically-calculated (Mie model) values for national parks in USA (Pitchford et al., 2007), would lead to large underestimation (9%) of the role of AN, while the total reconstructed extinction would be 30% of the light extinction observed. Finally, using a fairly comparable sampling site in Europe, MEE parameters derived through theoretical calculations on a filter analysis for $PM_{2.5}$ in the Po Valley (Valentini et al., 2018), would lead to an underestimation of the AS extinction by 6% which might be driven by the contribution of super micron aerosols (mainly sulfate and nitrate) to the PM mass concentration (for more details, please refer to Fig. S2 in the Supplementary Information).

4. Conclusion

Accurate knowledge of the physical, chemical and optical properties of aerosol particles is essential to reduce current uncertainties associated to their radiative impacts on Earth's climate. Nevertheless, the complex aerosol (trans)formation processes and range of sources lead to a strong spatial and temporal variability in aerosol properties. In this study, we combined in situ coincident aerosol chemical and physical measurements in PM_1 via the IMPROVE algorithm, to provide robust estimates of their optical properties relevant for better assessments on their role on climate.

The IMPROVE algorithm uses fixed MEE values for six major chemical species of PM. This method has been used for estimating the extinction coefficients mostly in the United States and China, whereas only a few studies have addressed this topic at south European sites in PM_{10} and $PM_{2.5}$, lacking information in polluted urban hotspots of northwestern European countries. Hence, in this study for the first time, we retrieved the light extinction and the composition-based apportionment in the smallest fraction of one of the most polluted northwestern Europe cities (Lille). First of all, we employed literature-based MEE reported for suburban and urban sites over ~3 years of measurements at ATOLL, where the light extinction reconstructed at 525 nm and the composition-based apportionment are retrieved with a range of biases depending on the chosen reference (e. g. overestimation of 70% reconstructed extinction using Cheng et al., 2008). Therefore, we used a multiple linear regression to derive specific multi-annual MEEs for ATOLL.

The multiannual analysis, using MEE derived from the multiple linear regression, highlights ammonium nitrate as the predominant species regarding the extinction at 525 nm (35%), followed by the carbonaceous aerosol species (eBC 29%, Org 21%) and ammonium sulfate (15%). Regarding the absorption at 370 nm, organics are responsible for 22% of the absorption, evidencing a significant contribution of Brown Carbon in the region. The extinction is shown to be generally higher during winter, strongly impacted by aerosol emissions related to solid fuel combustion from residential heating, and during spring, in which agricultural activities combined with traffic emissions (NOx) lead to strong ammonium nitrate formation.

Overall, this study provides new evidences that not considering aerosol heterogeneity among different sampling sites and seasons, can lead to significant biases in estimating their extinction. Our analysis of the long-term ATOLL dataset in Lille highlights the ability of retrieving robust aerosol optical properties from chemical composition measurements, constrained by coincident absorption and scattering measurements. In addition, this work supports the use of site-specific parameters (that reflect various influences, as mixing state, size distribution of aerosol components) along with long-term field observations, to derive key aerosol optical properties relevant for climate modelling and air quality assessment.

Author contributions

Conceptualization: JFB, SC, IC, VR; Data Curation: AVG, SC, VR; Formal analysis: AVG, JFB, SC; Funding acquisition: AVG, IC, VR; Investigation: AVG, JFB, SC, VR; Methodology: JFB, SC; Project administration: IC, VR; Resources: ET, EB, VR; Software: AVG, JFB, SC; Supervision: IC, VR; Validation: JFB, SC, ET, EB, VR; Visualization: AVG; Writing – Original Draft: AVG, JFB; Writing – Review & Editing: SC, IC, VR.

Funding sources

A. Velazquez Garcia's PhD grant is supported by CONACyT PhD grant (2019-000004-01EXTF-00001) and the Hauts-de-France Regional Council. IMT Nord Europe and LOA acknowledge financial support from the Labex CaPPA project, which is funded by the French National Research Agency (ANR) through the PIA (Programme d'Investissement d'Avenir) under contract ANR-11-LABX-0005-01, and the CLIMIBIO project, both financed by the Regional Council "Hauts-de-France" and the European Regional Development Fund (ERDF). IMT Nord Europe participated in the COST COLOSSAL Action CA16109. The ATOLL site is one of the French ACTRIS National Facilities and contributes to the CARA program of the LCSQA funded by the French Ministry of Environment.

Declaration of competing interest

The authors declare that they have no known competing financial interests or personal relationships that could have appeared to influence the work reported in this paper

Data availability

Data will be made available on request.

Acknowledgment

The authors are really grateful to the staff at LOA, in particular Prof. P. Goloub, F. Auriol and R. De Filippi, for supporting the technical and logistical implementation of the instruments, and to Dr. L.-H. Rivellini (now at Singapore National University) for her early involvement. We thank T. Podvin (LOA) for providing the weather data at ATOLL, and the air quality monitoring network Atmo Hauts-de-France for providing NO_2 concentrations at the Lille Fives monitoring station.

Appendix A. Supplementary data

Supplementary data to this article can be found online at https://doi.org/10.1016/j.atmosenv.2023.119613.

ABBREVIATIONS

ATOLL	ATmospheric Observations in liLLe
MEE	Mass Extinction Efficiency
MSE	Mass Scattering Efficiency
MAE	Mass Absorption Efficiency
IMPROVE	Interagency Monitoring of Protected Visual Environments
ACTRIS	The Aerosol, Clouds and Trace Gases Research Infrastructure
ACSM	Aerosol Chemical Speciation Monitor
AAE	Absorption Ångström exponent
SSA	Single Scattering Albedo
RS	Rayleigh scattering
T	Temperature
RH	Relative Humidity
Cj	Mass concentration of species j
f(RH)	Water growth function
AS	Ammonium Sulfate
AN	Ammonium Nitrate
Org	Organic fraction
BC	Black Carbon
FS	Fine Soil
SS	Sea Salt
MLR	Multiple Linear Regression
PM1	fine particles with an aerodynamic diameter less than 1 μm
NR-PM1	Non-Refractory PM1
eBC	equivalent Black carbon (for data derived from optical absorption methods)
σscat	Scattering Coefficient
σabs	Absorption Coefficient
σext	Extinction Coefficient
SIA	Secondary Inorganic Aerosols
GAW	Global Atmosphere Watch
IPR	Ispra, Po Valley, Italy (GAW site)

References

Bernardoni, V., et al., 2017. Size-segregated aerosol in a hot-spot pollution urban area: chemical composition and three-way source apportionment. Environ. Pollut. 231, 601–611.

Bodhaine, Barry A., Wood, Norman B., Dutton, Ellsworth G., Slusser, James R., 1999. On Rayleigh optical depth calculations. J. Atmos. Ocean. Technol. 16 (11), 1854–1861.

Chen, Xiaojia, et al., 2016. Reconstructed light extinction coefficients of fine particulate matter in rural guangzhou, southern China. Aerosol Air Qual. Res. 16 (8), 1981–1990.

Cheng, Y.F., et al., 2008. Aerosol optical properties and related chemical apportionment at xinken in Pearl River delta of China. Atmos. Environ. 42 (25), 6351–6372.

Cheng, Zhen, et al., 2015. Estimation of aerosol mass scattering efficiencies under high mass loading: case study for the megacity of shanghai, China. Environ. Sci. Technol. 49 (2), 831–838.

Crenn, V., Fronval, I., Petitprez, D., Riffault, V., 2017. Fine particles sampled at an urban background site and an industrialized coastal site in northern France — Part 1: seasonal variations and chemical characterization. Sci. Total Environ. 578, 203–218.

Crumeyrolle, Suzanne, et al., 2021. On the importance of nitrate for the droplet concentration in stratocumulus in the north-sea region. Atmos. Environ. 252, 118278.

Cuesta-Mosquera, Andrea, et al., 2021. Intercomparison and characterization of 23 aethalometers under laboratory and ambient air conditions: procedures and unit-to-unit variabilities. Atmos. Meas. Tech. 14 (4), 3195–3216.

Drinovec, L., et al., 2015. The 'Dual-Spot' Aethalometer: an Improved Measurement of Aerosol Black Carbon with Real-Time Loading Compensation. https://oar.tib.eu/jspui/handle/123456789/765. (Accessed 22 October 2020).

Favez, Olivier, et al., 2021. Overview of the French operational network for in situ observation of PM chemical composition and sources in urban environments (CARA program). Atmosphere 12 (2), 207.

Forster, Piers, et al., 2021. The Earth's energy budget, climate feedbacks, and climate sensitivity. In: Masson-Delmotte, Valérie, et al. (Eds.), Climate Change 2021: the Physical Science Basis. Contribution of Working Group I to the Sixth Assessment Report of the Intergovernmental Panel on Climate Change. Cambridge University Press.

Gómez-González, Y., et al., 2012. Chemical characterisation of atmospheric aerosols during a 2007 summer field campaign at brasschaat, Belgium: sources and source processes of biogenic secondary organic aerosol. Atmos. Chem. Phys. 12 (1), 125–138.

Groblicki, Peter J., Wolff, George T., Countess, Richard J., 1981. Visibility-reducing species in the denver 'Brown cloud'—I. Relationships between extinction and chemical composition. Atmos. Environ. 15 (12), 2473–2484, 1967.

Hand, J.L., Malm, W.C., 2007. Review of aerosol mass scattering efficiencies from ground-based measurements since 1990. J. Geophys. Res. Atmos. 112 (D16). https://agupubs.onlinelibrary.wiley.com/doi/abs/10.1029/2007JD008484. (Accessed 14 May 2020).

Laj, Paolo, et al., 2020. A global analysis of climate-relevant aerosol properties retrieved from the network of global atmosphere Watch (GAW) near-surface observatories. Atmos. Meas. Tech. 13 (8), 4353–4392.

Laskin, Alexander, Laskin, Julia, Sergey, A., Nizkorodov, 2015. Chemistry of atmospheric Brown carbon. Chem. Rev. 115 (10), 4335–4382.

Li, Lei, et al., 2019. Retrieval of aerosol components directly from satellite and ground-based measurements. Atmos. Chem. Phys. 19 (21), 13409–13443.

Malm, William C., et al., 1994. Spatial and seasonal trends in particle concentration and optical extinction in the United States. J. Geophys. Res. 99 (D1), 1347–1370.

Moschos, Vaios, et al., 2020. Source-specific light absorption by carbonaceous components in the complex aerosol matrix from yearly filter-based measurements. Atmos. Chem. Phys. Discuss. 1–44.

Müller, T., Laborde, M., Kassell, G., Wiedensohler, A., 2011. Design and performance of a three-wavelength LED-based total scatter and backscatter integrating nephelometer. Atmos. Meas. Tech. 4 (6), 1291–1303.

Myhre, G., et al., 2013. Radiative forcing of the direct aerosol effect from AeroCom Phase II simulations. Atmos. Chem. Phys. 13 (4), 1853–1877.

Ng, N.L., et al., 2011. Real-time methods for estimating organic component mass concentrations from aerosol mass spectrometer data. Environ. Sci. Technol. 45 (3), 910–916.

Pitchford, Marc, et al., 2007. Revised algorithm for estimating light extinction from IMPROVE particle speciation data. J. Air Waste Manag. Assoc. 57 (11), 1326–1336.

Qu, W.J., et al., 2015. Influence of relative humidity on aerosol composition: impacts on light extinction and visibility impairment at two sites in coastal area of China. Atmos. Res. 153, 500–511.

Rodelas, Roig, Roger, Esperanza Perdrix, Herbin, Benoît, Riffault, Véronique, 2019. Characterization and variability of inorganic aerosols and their gaseous precursors at a suburban site in northern France over one year (2015–2016). Atmos. Environ. 200, 142–157.

Sciare, J., et al., 2005. Aerosol mass closure and reconstruction of the light scattering coefficient over the eastern mediterranean sea during the MINOS campaign. Atmos. Chem. Phys. 5 (8), 2253–2265.

Seinfeld, John H., Pandis, Spyros N., 2012. Atmospheric Chemistry and Physics: from Air Pollution to Climate Change. John Wiley & Sons.

Tao, Jun, et al., 2014. Impact of PM2.5 chemical compositions on aerosol light scattering in guangzhou — the largest megacity in south China. Atmos. Res. 135–136, 48–58.

Tao, Jun, Zhang, Leiming, Wu, Yunfei, Zhang, Zhisheng, 2020. Evaluation of the IMPROVE formulas based on mie model in the calculation of particle scattering coefficient in an urban atmosphere. Atmos. Environ. 222, 117116.

Titos, G., et al., 2012. Optical properties and chemical composition of aerosol particles at an urban location: an estimation of the aerosol mass scattering and absorption efficiencies. J. Geophys. Res. Atmos. 117 (D4). https://agupubs.onlinelibrary.wiley.com/doi/abs/10.1029/2011JD016671. (Accessed 23 October 2020).

Valentini, S., et al., 2018. Tailored coefficients in the algorithm to assess reconstructed light extinction at urban sites: a comparison with the improve revised approach. Atmos. Environ. 172, 168–176.

Vecchi, R., et al., 2018. Assessment of light extinction at a European polluted urban area during wintertime: impact of PM1 composition and sources. Environ. Pollut. 233, 679–689.
Waked, Antoine, et al., 2018. Investigation of the geographical origins of PM10 based on long, medium and short-range air mass back-trajectories impacting northern France during the period 2009–2013. Atmos. Environ. 193, 143–152.
Wang, Huanbo, et al., 2015a. Chemical composition and light extinction contribution of PM2.5 in urban beijing for a 1-year period. Aerosol Air Qual. Res. 15 (6), 2200–2211.
Wang, Qingqing, et al., 2015b. Chemical composition of aerosol particles and light extinction apportionment before and during the heating season in beijing, China. J. Geophys. Res. Atmos. 120 (24), 12708–12722.
Wang, Shuo, et al., 2021. Real-time retrieval of aerosol chemical composition using effective density and the imaginary part of complex refractive index. Atmos. Environ. 245, 117959.
Wilcox, E.M., 2012. Direct and semi-direct radiative forcing of smoke aerosols over clouds. Atmos. Chem. Phys. 12 (1), 139–149.
Xia, Yunjie, et al., 2017. Impact of size distributions of major chemical components in fine particles on light extinction in urban guangzhou. Sci. Total Environ. 587–588, 240–247.
Yao, TingTing, et al., 2010. High time resolution observation and statistical analysis of atmospheric light extinction properties and the chemical speciation of fine particulates. Sci. China Chem. 53 (8), 1801–1808.
Yu, H., Wu, C., Wu, D., Yu, J.Z., 2010. Size distributions of elemental carbon and its contribution to light extinction in urban and rural locations in the Pearl River delta region, China. Atmos. Chem. Phys. 10 (11), 5107–5119.
Zhang, Shouwen, et al., 2021. Near real-time PM1 chemical composition measurements at a French urban background and coastal site under industrial influence over more than a year: temporal variability and assessment of sulfur-containing emissions. Atmos. Environ. 244, 117960.
Zhang, Yunjiang, et al., 2020. Substantial Brown carbon emissions from wintertime residential wood burning over France. Sci. Total Environ. 743, 140752.
Zhou, Yaqing, et al., 2019. Exploring the impact of chemical composition on aerosol light extinction during winter in a heavily polluted urban area of China. J. Environ. Manag. 247, 766–775.